FUDMA Journal of Sciences (FJS)
ISSN online: 2616-1370
ISSN print: 2645 - 2944
Vol. 9 No. 12, December (Special Issue), 2025, pp 725 – 740
DOI: https://doi.org/10.33003/fjs-2025-0912-4388

GRAIN SIZE AND PEBBLE MORPHOMETRY OF BIDA FORMATION SANDSTONES (NORTHERN BIDA BASIN): IMPLICATIONS FOR SEDIMENTARY PROCESSES

[1]Jimoh A. Yusuf, [1]Arinde A. Victoria, [2]Ojo J. Olusola, [3]Haruna K. Abdulrazaq and [4]Nurudeen K. Olasunkanmi

[1]Department of Geology and Mineral Science, Faculty of Pure and Applied Sciences, Kwara State University, Malete, Kwara State, Nigeria.
[2]Department of Geology, Federal University Oye -Ekiti, Ekiti State, Nigeria.
[3]Department of Chemical and Geological Sciences, Al-Hikmah University, Ilorin, Kwara State, Nigeria.
[4]Department of Physics and Material Science, Faculty of Pure and Applied Sciences, Kwara State University, Malete, Kwara State, Nigeria.

*Corresponding authors' email: yusuf.jimoh@kwasu.edu.ng
ORCID: http://orcid.org/0000-0002-7013-996X

ABSTRACT

The intracratonic Bida Basin is one of the inland sedimentary basin in Nigeria with clastic deposition. This study investigates the transportation history, maturity, and paleodepositional environments of the Cretaceous sandstones from the Bida Formation exposed at Gbugbu, Ndeji, Maganiko, and Lafiagi within the Northern Bida Basin. A sedimentological approach was employed, comprising grain size analysis (n=26) and pebble morphometry (n=149). The inclusive graphic standard deviation (sorting) values range from (1.00-1.19, 1.28-1.98, 1.04-1.28, and 0.89-1.42) respectively, indicating most of the sandstones are poorly sorted. The sandstones, especially at Gbugbu, Maganiko, and Lafiagi, are fine-skewed to near-symmetrical, while the sandstones at Ndeji are coarse-skewed. The majority of the sandstones are platykurtic with values ranging from (0.75-0.94). These variations in the sorting, skewness, and kurtosis indicate fluctuating depositional energy, mixed sources, short transportation, and environments ranging from fluvial dominance over beach settings. Morphometry indices such as the mean, flatness ratio, elongation ratio, oblate-prolate index, and maximum projection sphericity index support these environmental interpretations, with sphericity values ≥ 0.65 suggesting fluvial dominance. The roundness and sphericity of the pebbles suggest short transportation. The occurrence of beach pebbles in the Bida Formation is an indication that the sediments were deposited in an environment shared between a river and beach tidal zone since the majority of pebbles showed a bladed form in the sphericity-form diagram. The majority of the pebbles yielded a bladed compact shape with a dominating sphericity index symptomatic of fluvial sediments. In conclusion, the study indicates a sedimentary system characterized by a fluctuating depositional system dominated by variable fluvial, wave processes and significant environmental variability across the study area.

Keywords: Bida, Fluvial, Sandstone, Paleoenvironment

INTRODUCTION

The Bida Basin (Figure 1) is a rift basin and one of the inland sedimentary basins in Nigeria with clastic sediments of about 4km, located at the north central part of Nigeria (Udenzi and Osazuwa, 2004). It is a northwest-southeast trending intracratonic structural depression adjacent and contiguous with Sokoto and Anambra Basins in the northwest and southeast respectively. The basin is divided into two geographic regions, namely the northern and southern Bida basins (Braide, 1992a). The Northern Bida Basin, part of the Cretaceous sedimentary successions of central Nigeria, presents an ideal setting for investigating sediment provenance, transport dynamics, and paleoenvironmental evolution. The Bida Basin is underlain by a Precambrian basement complex, which consists of crystalline rocks and older metamorphic formations. These basement rocks provide the foundational structure upon which subsequent sedimentary layers accumulate. During the Middle Jurassic to Early Cretaceous, rifting occurred, in which the extension created several horst and graben structures with reactivation phases during the middle to late Cretaceous. The comprehensive account of the geologic sequence of the northern Bida Basin have been documented in literature (Agyingi, 1993; Ojo and Akande, 2006; Ojo, 2012). The Campanian Bida Formation is the oldest stratigraphic unit in the northern Bida Basin comprising of conglomerate and sandstones, and is the lateral equivalent to the Lokoja Formation in the southern Bida basin. The Sakpe Ironstone, Enagi Formation (sandstone, siltstone, claystone) and Batati Ironstone Formation in chronological order, makes up the remaining units in the northern Bida Basin and their lateral equivalent are the Patti Formation (sandstone, shale, claystone) and Agbaja Formation (ironstone) (Figure 2).

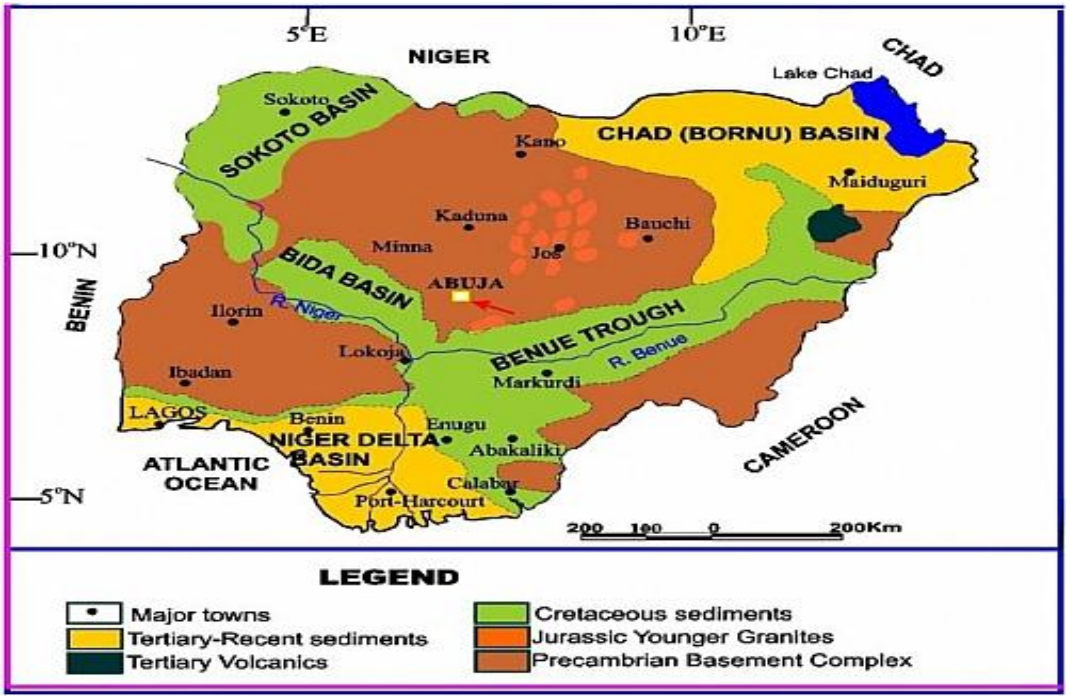

Figure 1: Geological Map of Nigeria Showing the Sedimentary Basins and the Basin of Interest (Bida Basin) Modified after (Obaje *et al.* 2004)

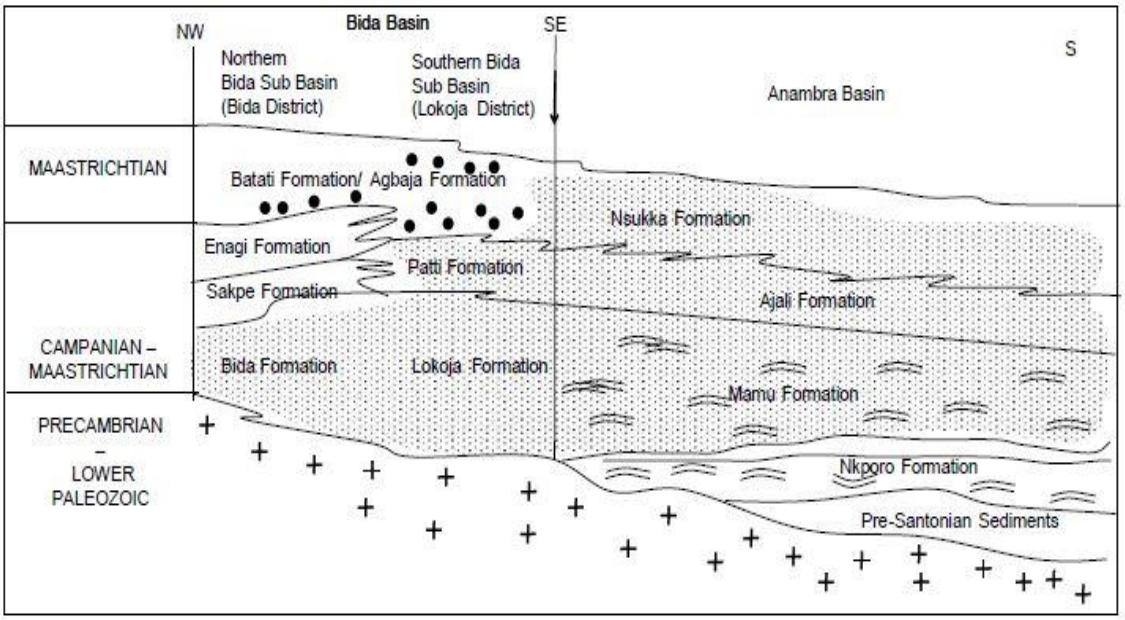

Figure 2: Generalized Stratigraphy of the Bida Basin Showing the Bida Formation After (Ojo *et al.* 2021).

In recent years, there has been a growing interest in understanding the mineral resource potential, depositional style, and paleogeographic framework of the Bida Basin, with particular attention directed toward its southern segment due to the potential source rock for hydrocarbon generation. Several studies have addressed various aspects of the basin's geology. For instance, Braide (1992a), Idowu and Enu (1992), Ojo and Akande (2003, 2009), Obaje *et al.* (2004), Akande et al. (2005), Ojo *et al.* (2020, 2021); Ayuba *et al.* (2024), Ojoma *et al*. (2024), Bamidele and Ojo (2025), and Ojo *et al.* (2026) have provided insights into the sedimentary characteristics and stratigraphy of the southern part of the Bida Basin. In contrast, investigations in the northern part of the basin have focused on sedimentology and depositional settings. Notable contributions include those by Adeleye (1974), Braide (1992b), Olaniyan and Olobaniyi (1996), Olugbemiro and Nwajide (1997). Ojo, (2012) analyzed pebble morphology, grain size trends, and facies architecture of the clastic deposits and concluded a fluvial origin for the sandstones and conglomerates in the study area. A comprehensive understanding of source and reservoir rock potential, as well as mineral prospectivity in this underexplored inland basin, requires detailed reconstruction of sediment provenance and depositional history. Achieving this necessitates measuring stratigraphic sections, detailed lithofacies descriptions, systematic sampling, grain size analysis and pebble morphometry studies. This study focuses on exposures at Gbugbu (GB), Ndeji (ND), Maganiko (MG),

and Lafiagi (LF) using grain size analysis and pebble morphometry. To date, few integrated studies have been undertaken in the northern part of the basin, particularly south of the Niger River. This study addresses this gap by focusing on the Gbugbu–Lafiaji areas (Figure 3), employing outcrop field sampling to achieve the following objectives: (1) reconstruct the paleodepositional environments of the sediments; (2) assess their textural characteristics and transportation mechanisms; and (3) evaluate the sorting and maturity of the sandstones.

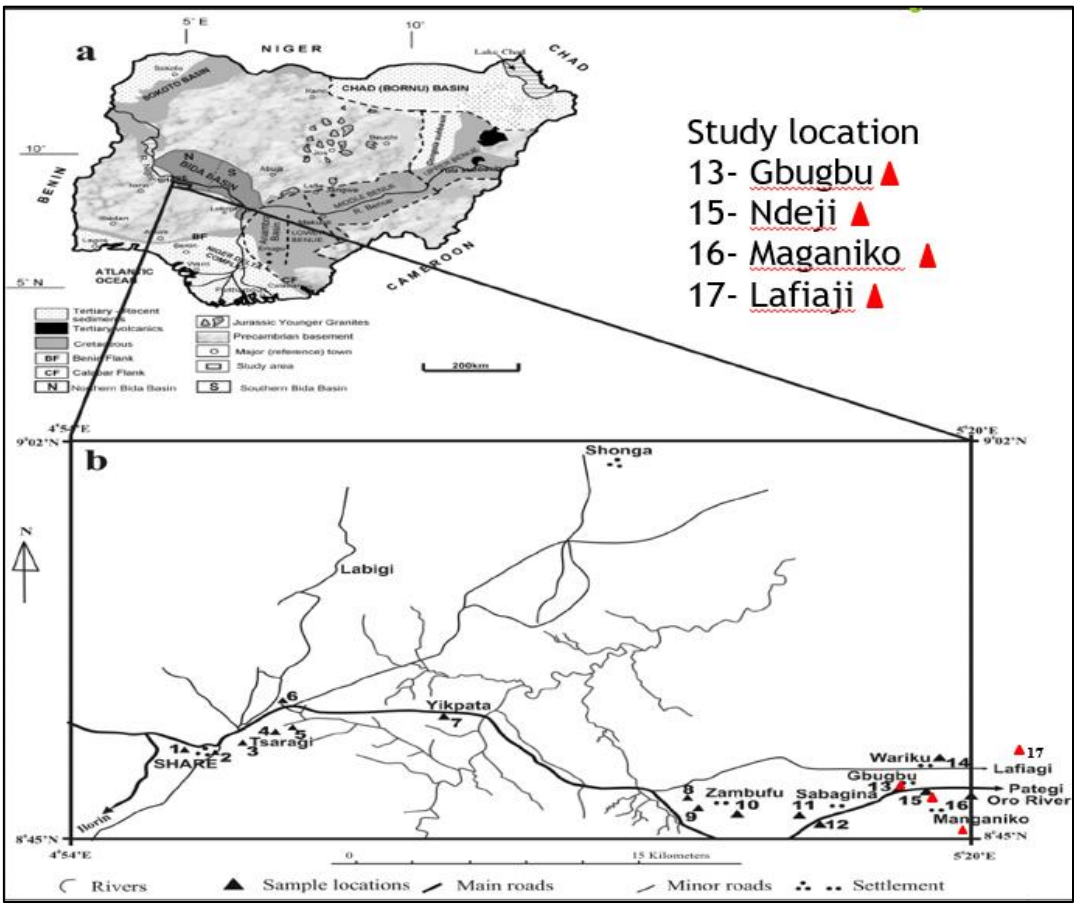

Figure 3: Location Map of the Study Areas Modified After (Ojo, 2012)

MATERIALS AND METHODS

Fieldwork was conducted in Gbugbu, Ndeji, Maganiko, and Lafiagi areas (Figure 3) of the Bida Basin to investigate sedimentological characteristics. It began with reconnaissance surveys to identify key outcrops using topographic and geological maps. Vertical stratigraphic profiles were developed for each location to document changes in sediment texture, thickness, and sedimentary structures. These profiles were constructed through detailed bed-by-bed logging and lithological description (Figures 4, 5, 6 and 7). The precise geographic coordinates of the outcrop sites were recorded using a handheld GPS device. Representative sandstone samples (n=26) were collected for mechanical grain size analysis, with textural parameters determined following the methodology of Folk and Ward (1957). Additionally, clasts from conglomeratic sandstone units ranging from pebbles to cobbles were randomly selected for pebble morphometric analysis (n=149). Each clast's three principal axes (long, intermediate, and short) were measured using a digital vernier caliper, following the approach of Stratten (1973). Morphometric indices such as Flatness Ratio (FR) and Elongation Ratio (ER) were calculated according to Luttig (1962) and Dobkins & Folk (1970), while the Oblate–Prolate Index (OPI) and Maximum Projection Sphericity Index (MPSI) were derived using the equations proposed by Sneed and Folk (1958).

RESULTS AND DISCUSSION

Lithological Description

A sequence of coarse siliciclastic sediments, ranging from massive pebbly sandstone at the base to medium-coarse grained sandstones in the upper part of the section was recorded in the lithologic succession at Gbugbu (Figures 4, 8a). Deposition in a high-energy fluvial system is generally reflected in the log. The massive, coarse, pebbly sandstone that makes up the basal unit is thought to be a channel-lag deposit that was formed under extremely high energy conditions. A conglomeratic sandstone that represents residual gravel-bar or channel-floor accumulation overlies the pebbly sandstone. The brownish to greyish medium-grained clayey sandstones on top show a shift toward decreased flow energy. Periodic suspension settling is implied by the higher fines during these intervals. After that, the succession moves upward into massive, moderately to poorly sorted, coarser reddish-brown sandstones. The predominance of coarse-grained sediments in the section underscores the proximity of the study site to the main fluvial channel belt and suggests deposition relatively close to sediment sources within a continental alluvial setting.

At Ndeji, the predominance of coarse-grained sediments highlights the study area's close proximity to the main fluvial channel belt and indicates that deposition occurred relatively close to sediment sources in a continental setting (Figures 5,

8b). The reddish sandstones in the basal interval is fine-grained and well-compacted, indicating low-to-moderate energy deposition. A medium-to-coarse-grained pinkish sandstone with parallel-laminated and bioturbated intervals overlies this interval. Primary lamination and the ensuing biogenic disturbance point to alternating traction transport periods interspersed with quieter conditions that allowed biogenic structure to form. Conglomeratic units and extremely coarse brownish sandstone overlying the conglomerates representing repeated phases of high-energy channel reactivation. Overall, the succession shows an upward trend from moderately energetic sandy facies to very high-energy conglomeratic facies, which is indicative of migration or channel deepening over time. The frequent reoccupation of the area by an active river channel, most likely within a braided or gravel-bed fluvial system, is indicated by the repeated stacking of sandstones and conglomerates.

A 1.93m thick unit of sandstone with a distinct vertical gradation in grain size and composition is described by the logged sequence at Maganiko (Figures 6, 8c). The unit is consistently described as "Mottled," indicating a fluctuating color pattern that is usually the result of weathering, oxidation, and pedogenic (soil-forming) processes. A period of increasing flow energy in the depositional environment is suggested by the progression from medium-grained sandstone at the base to a conglomeratic, iron-rich sandstone at the upper part of the log, which shows a coarsening-upward sequence. The section documents a dynamic sedimentary history that started with the moderate-energy deposition of sandy sediments, changed to a high-energy environment where gravel was deposited, and ended with a period of subaerial exposure and chemical weathering that resulted in the formation of a resistant, iron-cemented cap.

The log at Lafiaji present a 5.2m succession of terrigenous clastic rocks, predominantly sandstone, with a consistent reddish color indicating oxidation (Figure 7, 8d). The sequence is divided into ten distinct lithofacies (LF1 to LF10), revealing a dynamic depositional and post-depositional history. The overall sequence shows a general coarsening-upward trend, beginning with fine to medium-grained, clayey sandstone at the base (LF1) and culminating in massive, coarse-grained sandstone at the top (LF10). A significant characteristic of the middle section (LF3 to LF6) is pervasive ferruginization (cementation by iron oxides). The upper part of the sequence (LF7 to LF9) shows evidence of biological activity in the form of bioturbation (burrows). The coarsening-upward trend, presence of parallel lamination (LF4), and overall sandstone composition are highly suggestive of a fluvial (river). The sequence could represent a gradual infilling of a channel or basin with increasingly coarse sediment.

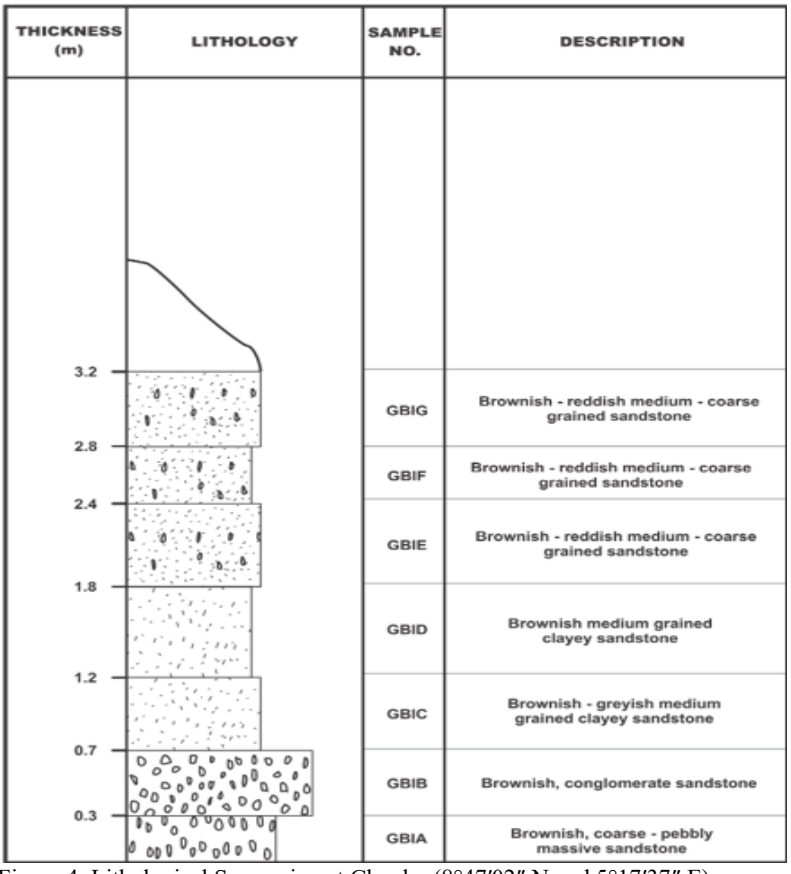

Figure 4: Lithological Succession at Gbugbu (8°47′02″ N and 5°17′37″ E)

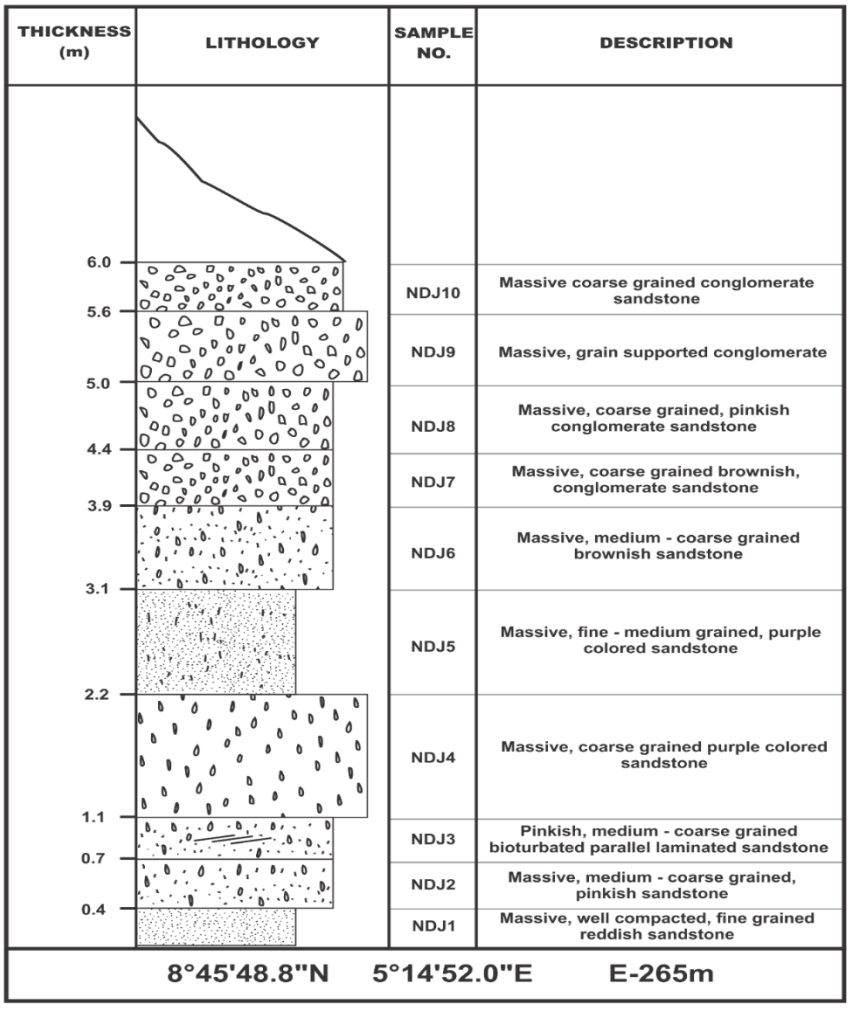

Figure 5: Lithological Succession at Ndeji

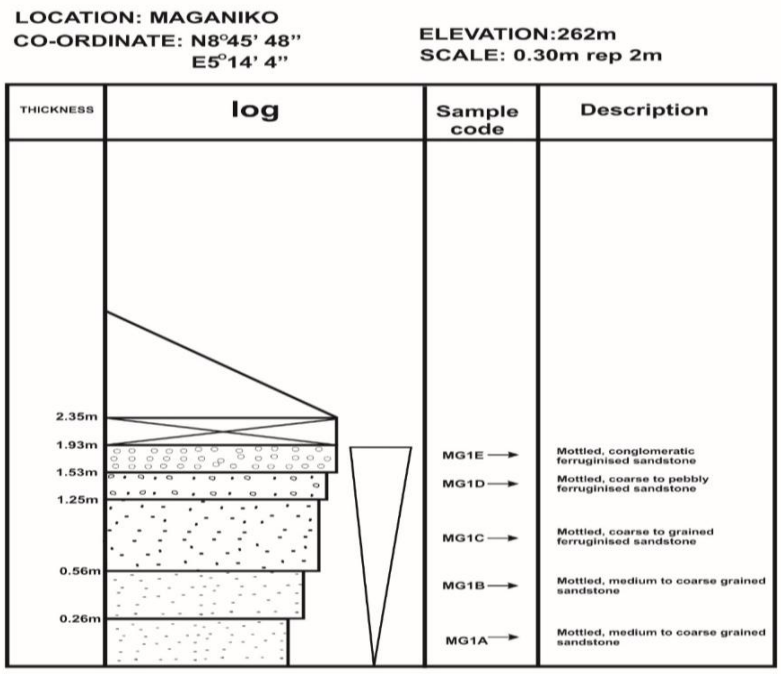

Figure 6: Lithological Succession at Maganiko

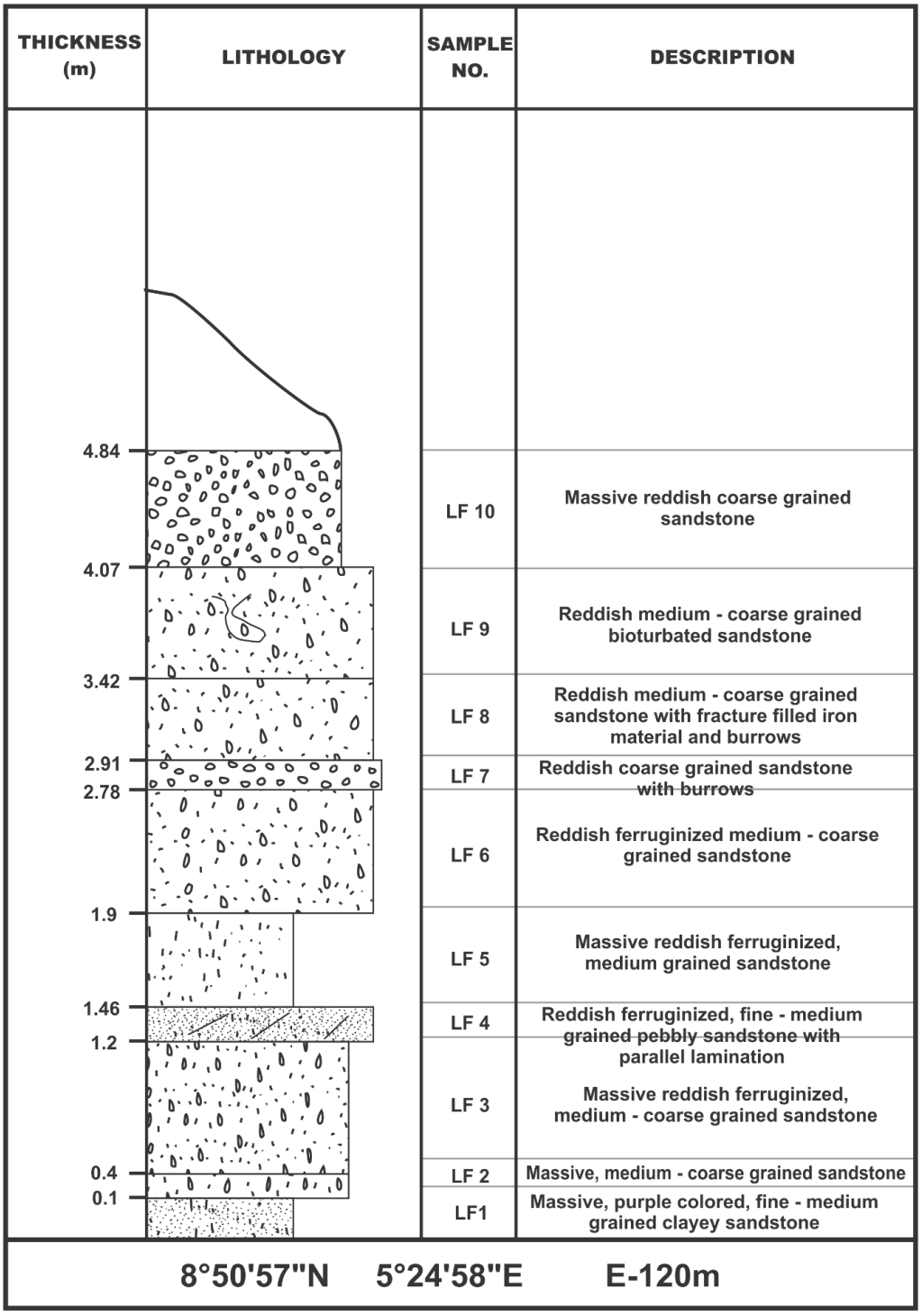

Figure 7: Lithological Succession at Lafiaji

(a) (b) (c) (d)

Figure 8: (a) Conglomeratic Sandstone Facies at Gbugbu, (b) Medium-Coarse Grained Sandstone Facie at Ndeji, (c) Mottled Medium Grained Sandstone facie at Maganiko (d) Reddish Coarse Grained Sandstone Facie at Lafiaji

Grain Size Data

The grain size analyses provide key insights into the sedimentological characteristics of the sandstone units within the study area. The results of the grain size analysis of the sandstones were used to compute the textural parameters such as mean, standard deviation (sorting), skewness and kurtosis (Table 1). These parameters aid in interpreting depositional energy, sediment transport, and sorting levels. The mean size ranges from (3.74-4.37 ϕ), (3.45-3.78 ϕ), (4.07-4.80 ϕ), and (-0.4 to - 0.17ϕ) for Lafiaji, Gbugbu, Maganiko and Ndeji samples, respectively. The standard deviation (sorting) ranges from (0.89 -1.42ϕ), (1.00-1.19ϕ), (1.18-1.28ϕ), and (1.28-1.98ϕ) respectively. For the skewness, the values are (-0.12 – 0.18ϕ), (0.03-0.15ϕ), (0.09-0.11ϕ), and (-0.45 to – 0.25ϕ) (Table 2). The Kurtosis ranges from (0.80 – 0.94ϕ), (0.85 – 0.93ϕ), (0.86 – 0.88ϕ), and (0.75-0.82ϕ) for the locations, respectively.

Grain Size, Sorting and Transportation Mechanism

The positive mean size of the samples (Table 1) indicates that the samples from Lafiaji (LF), Gbugbu (GB) and Maganiko (MG) are fine – medium grained sandstones. This is supported by the positive skewness values (fine skewed - near symmetrical) for the samples for these locations. The Ndeji (ND) samples exhibit negative mean size and skewness (coarse skewed) pointing to more coarser grains. Most of the samples denoted by LF, GB, and MG are poorly sorted with a few samples exhibiting moderate sorting. The ND samples are specifically very poorly sorted (Table 1 & 2). This observation is consistent with the work of (Ojo, 2012). The poor sorting indicates variable flow velocities/rapid deposition as well as short distance river transportation of the sediments. The poor sorting and positive skewness suggest fluvial environments for the sandstones (Tucker, 1988; Ojo, 2012; Madi & Ndlanzi, 2020). The poor sorting and positive skewness are characteristics of fluvial system marked by inconsistent current in a moderate energy environment with a periodic low energy phases allowing fine particles to settle (Selley, 1985; Tucker, 1988; Amajor & Ngerebara, 1990; Ojo, 2012). The LF, GB and MG samples indicates stable but slightly fluctuating flow regimes while the ND samples suggest rapid deposition with minimal transport in a high-energy environments (debris flows) with minimal reworking due to the extremely poor sorting. All the samples exhibit platykurtic (flat peak) indicating mixing sediments sources. The bivariate plots of Friedman (1967, 1979) mean vs. sorting, kurtosis vs. skewness shows that LF, GB and MG samples are fine grains, fine skewed – near symmetrical, and poorly sorted (Figure 9 & 10) while the ND samples are coarse grained, very coarse skewed and very poorly sorted.

Pebble Morphometry: Implications for Paleoenvironmental Reconstruction

Pebble Morphometry analysis were conducted on 149 samples across the four locations and the results are presented in Tables 3, 4, 5 and 6. The significant range in clast sizes indicates that the conglomeratic sandstone are poorly sorted and lack compositional maturity. Most of the clasts are composed of quartz, with additional constituents including feldspar and rock fragments derived from meta-igneous rocks within the Basement Complex. Scatter diagrams e.g MPSI vs OPI, FR vs MPSI (Figure 11 and 12) were plotted using the coefficient of flatness, sphericity, Maximum Projection Sphericity Index, and the Oblate–Prolate Index to help differentiate depositional environments, following the methods of Dobkins & Folk (1970), Stratten (1973), and Nwajide & Hoque (1982). The majority of the samples are situated within the low-energy fluvial field, with only a few plotting in the high-energy beach environment (Figure 11 and 12). These plots help compare pebble shapes, sediment textures, and transport histories across the locations. Clustering in the plots may suggest similar depositional environments, while scattered patterns indicate varying energy conditions or sediment sources.

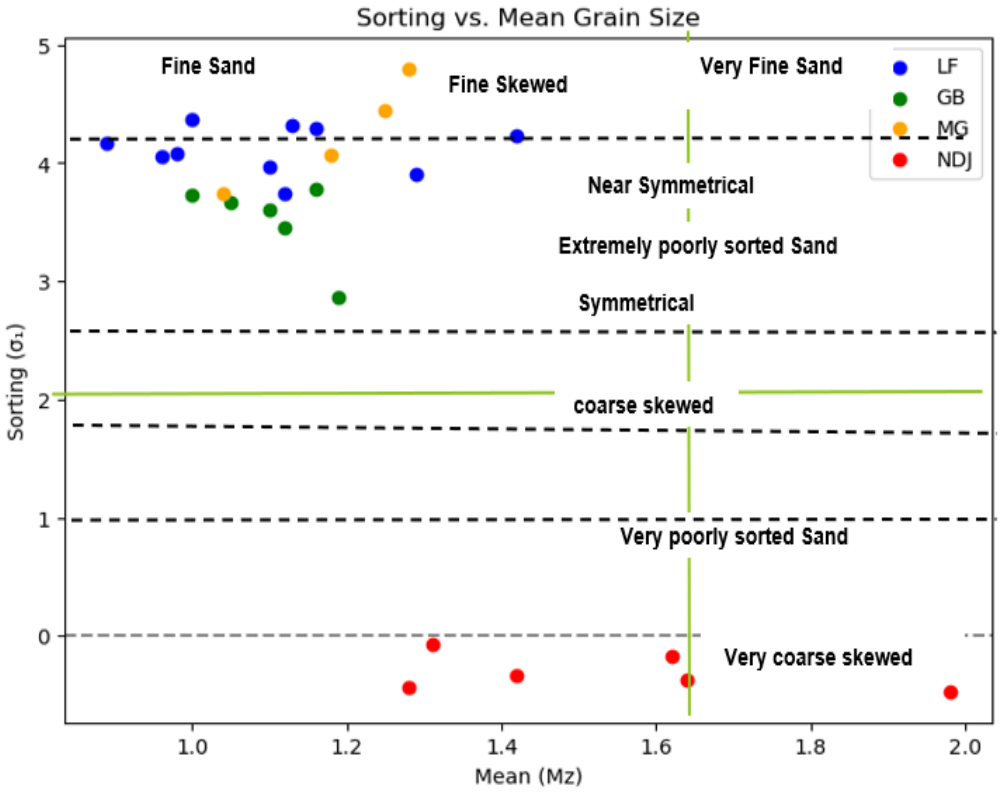

Figure 9: Plot of Sorting vs. Mean

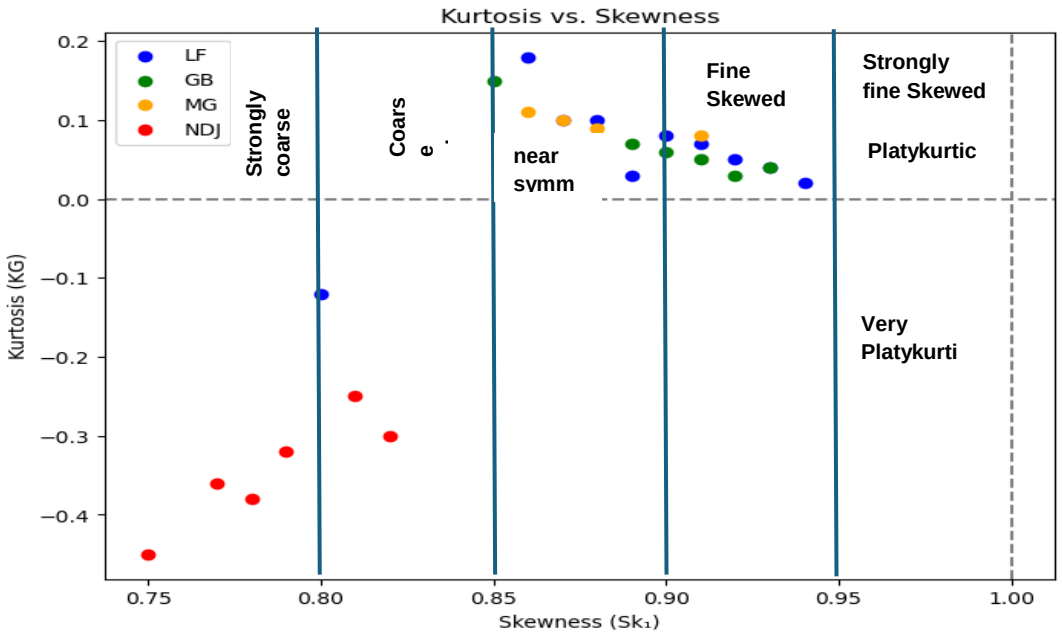

Figure 10: Plot of Kurtosis vs. Skewness

Samples with low flatness and MPSI values (<0.66) suggest high-energy beach environments, where intense wave action produces flatter, less spherical pebbles. In contrast, samples with MPSI >0.65 and flatness >50% indicate deposition in lower-energy fluvial settings, reflecting gentler, sustained transport and better rounding. Dobkins & Folk (1970) also suggested that the 0.66 sphericity line separate beach and river samples; whereas values lower than 0.66 are indicative of beach, and values higher than 0.66 indicate fluvial processes. The plots of MPSI against OPI (Figure 11), further distinguishes pebble forms: pebbles to the left of OPI = 0 and above MPSI = 0.65 represent prolate, high-sphericity forms typical of beach environments, while those to the right are more oblate and fluvially influenced. The pebbles and cobbles from LF, GB, MG, and ND samples have (50%, 61%, 58% and 91%) respectively fall within the fluvial settings while (50%, 39%, 42% and 9%) were deposited in the Beach settings (Table 3, 4, 5 and 6, Figure 11 and 12). The spread of samples across both plots reflects a range of depositional energies, confirming a continuum between beach and fluvial regimes (Figure 12). These patterns align with sediments deposited in an environment shared between river and beach tidal zone.

Table 1: Mean, Sorting, Skewness and Kurtosis Values Calculated from the Phi-Values for the Samples Analyzed

S/N	Sample	Mean (Mz)	Sorting (σ_1)	Skewness (Sk_1)	Kurtosis (KG)	Interpretation
1	LF1	4.17	0.89	0.05 (Near Symm)	0.92 (Platykurtic)	Moderately sorted, slightly fine-skewed
2	LF2	4.30	1.16	0.18 (Fine-skewed)	0.86 (Platykurtic)	Poorly sorted, fine-skewed
3	LF3	3.97	1.10	0.08 (Fine-skewed)	0.90 (Platykurtic)	Poorly sorted, slightly fine-skewed
4	LF4	4.05	0.96	0.02 (Near Symm)	0.94 (Platykurtic)	Moderately sorted, near symmetrical
5	LF5	4.37	1.00	0.10 (Fine-skewed)	0.88 (Platykurtic)	Poorly sorted, fine-skewed
6	LF6	4.23	1.42	-0.12 (Coarse-skewed)	0.80 (Platykurtic)	Very poorly sorted, coarse-skewed
7	LF7	4.32	1.13	0.10 (Fine-skewed)	0.87 (Platykurtic)	Poorly sorted, fine-skewed
8	LF8	3.90	1.29	0.03 (Near Symm)	0.89 (Platykurtic)	Poorly sorted, near symmetrical
9	LF9	3.74	1.12	0.07 (Fine-skewed)	0.91 (Platykurtic)	Poorly sorted, slightly fine-skewed
10	LF10	4.08	0.98	0.04 (Near Symm)	0.93 (Platykurtic)	Moderately sorted, near symmetrical
11	GB1A	3.78	1.16	0.07 (Fine-skewed)	0.89 (Platykurtic)	Poorly sorted, slightly fine-skewed
12	GB1G	2.87	1.19	0.15 (Fine-skewed)	0.85 (Platykurtic)	Poorly sorted, fine-skewed
13	GB1C	3.45	1.12	0.06 (Fine-skewed)	0.90 (Platykurtic)	Poorly sorted, slightly fine-skewed

S/N	Sample	Mean (Mz)	Sorting (σ_1)	Skewness (Sk_1)	Kurtosis (KG)	Interpretation
14	GB1E	3.73	1.00	0.04 (Near Symm)	0.93 (Platykurtic)	Moderately sorted, near symmetrical
15	GB1F	3.60	1.10	0.05 (Near Symm)	0.91 (Platykurtic)	Poorly sorted, near symmetrical
16	GB1D	3.67	1.05	0.03 (Near Symm)	0.92 (Platykurtic)	Poorly sorted, near symmetrical
17	MG1B	3.74	1.04	0.08 (Fine-skewed)	0.91 (Platykurtic)	Poorly sorted, slightly fine-skewed
18	MG1D	4.44	1.25	0.10 (Fine-skewed)	0.87 (Platykurtic)	Poorly sorted, fine-skewed
19	MG1C	4.80	1.28	0.11 (Fine-skewed)	0.86 (Platykurtic)	Poorly sorted, fine-skewed
20	MG1A	4.07	1.18	0.09 (Fine-skewed)	0.88 (Platykurtic)	Poorly sorted, fine-skewed
21	NDJ1A	-0.47	1.98	-0.45 (Coarse-skewed)	0.75 (Platykurtic)	Very poorly sorted, strongly coarse-skewed
22	NDJ1D	-0.43	1.28	-0.30 (Coarse-skewed)	0.82 (Platykurtic)	Poorly sorted, coarse-skewed
23	NDJ1F	-0.37	1.64	-0.38 (Coarse-skewed)	0.78 (Platykurtic)	Very poorly sorted, coarse-skewed
24	NDJ1G	-0.07	1.31	-0.25 (Coarse-skewed)	0.81 (Platykurtic)	Poorly sorted, coarse-skewed
25	NDJ1H	-0.33	1.42	-0.32 (Coarse-skewed)	0.79 (Platykurtic)	Very poorly sorted, coarse-skewed
26	NDJ1K	-0.17	1.62	-0.36 (Coarse-skewed)	0.77 (Platykurtic)	Very poorly sorted, coarse-skewed

Table 2: Summary of the Mean, Sorting, Skewness and Kurtosis for the Samples Analyzed

Location	Mean (Mz)	Sorting (σ_1)	Skewness (Ski)	Kurtosis (KG)	Interpretation Summary
Lafiagi (LF)	3.74 – 4.37	0.89 – 1.42	-0.12 (Coarse) to 0.18 (Fine)	0.80 – 0.94 (Platykurtic)	Moderately to poorly sorted; near symmetrical to fine-skewed; platykurtic
Gbugbu (GB)	3.45 – 3.78	1.00 – 1.19	0.03 – 0.15 (Fine)	0.85 – 0.93 (Platykurtic)	Poorly sorted; slightly fine-skewed to near symmetrical; platykurtic
Maganiko (MG)	4.07 – 4.80	1.18 – 1.28	0.09 – 0.11 (Fine)	0.86 – 0.88 (Platykurtic)	Poorly sorted; fine-skewed; platykurtic
Ndeji (ND)	-0.47 – -0.17	1.28 – 1.98	-0.45 – -0.25 (Coarse)	0.75 – 0.82 (Platykurtic)	Very poorly sorted; coarse-skewed; platykurtic

Table 3: Pebble Morphometric Data of Samples from Lafiaji

PEBBLE No	L(mm)	I(mm)	S(mm)	Mean (mm)	Flatness Ratio(S/L)	Elongation Ratio(I/L)	S/I	(L-I)/(L-S)	Flatness %	OPI	MPSI	Roundness	Sphericity	Depositional Environment
LF-1	60.1	41.6	27.9	43.2	0.464	0.692	0.671	0.575	46.423	-14.907	0.678	0.8	0.7	Fluvial
LF-2	47.5	36.1	19.1	34.233	0.402	0.76	0.529	0.401	40.211	19.718	0.597	0.9	0.6	Beach
LF-3	83.6	43.8	26.8	51.4	0.321	0.524	0.612	0.701	32.057	-40.141	0.581	0.7	0.6	Beach
LF-4	67.9	38.9	20.3	42.367	0.299	0.573	0.522	0.609	29.897	-21.849	0.538	0.7	0.6	Beach
LF-5	92.3	58.2	56.3	68.933	0.61	0.631	0.967	0.947	60.997	-89.444	0.839	0.7	0.8	Fluvial
LF-6	75.6	42.8	41.2	53.2	0.545	0.566	0.963	0.953	54.497	-90.698	0.807	0.7	0.8	Fluvial
LF-7	68	38.8	16	40.933	0.235	0.571	0.412	0.562	23.529	-12.308	0.46	0.7	0.5	Beach
LF-8	35.6	34.6	14.2	28.133	0.399	0.972	0.41	0.047	39.888	90.654	0.547	0.9	0.6	Beach
LF-9	47.9	32.7	26.3	35.633	0.549	0.683	0.804	0.704	54.906	-40.741	0.762	0.7	0.7	Fluvial
LF-10	60.9	33.7	18.7	37.767	0.307	0.553	0.555	0.645	30.706	-28.91	0.554	0.9	0.6	Beach
LF-11	34	28.2	17.4	26.533	0.512	0.829	0.617	0.349	51.176	30.12	0.681	0.8	0.7	Fluvial
LF-12	46.4	28.8	17.2	30.8	0.371	0.621	0.597	0.603	37.069	-20.548	0.605	0.7	0.6	Beach
LF-13	42.3	42.2	17.3	33.933	0.409	0.998	0.41	0.004	40.898	99.2	0.551	0.6	0.6	Beach
LF-14	37.1	34.9	20.1	30.7	0.542	0.941	0.576	0.129	54.178	74.118	0.678	0.6	0.7	Fluvial
LF-15	58.1	38.6	12.4	36.367	0.213	0.664	0.321	0.427	21.343	14.661	0.409	0.8	0.5	Beach
LF-16	55.1	36.2	15.9	35.733	0.289	0.657	0.439	0.482	28.857	3.571	0.502	0.7	0.5	Beach
LF-17	56.6	26.5	25.4	36.167	0.449	0.468	0.958	0.965	44.876	-92.949	0.755	0.6	0.7	Fluvial
LF-18	44.3	38.3	24.6	35.733	0.555	0.865	0.642	0.305	55.53	39.086	0.709	0.7	0.7	Fluvial
LF-19	39.7	30.1	14.7	28.167	0.37	0.758	0.488	0.384	37.028	23.2	0.565	0.7	0.6	Beach
LF-20	41.7	29.2	28.1	33	0.674	0.7	0.962	0.919	67.386	-83.824	0.866	0.6	0.8	Fluvial
LF-21	36.8	32.5	16.5	28.6	0.448	0.883	0.508	0.212	44.837	57.635	0.611	0.6	0.6	Beach

PEBBLE No	L(mm)	I(mm)	S(mm)	Mean (mm)	Flatness Ratio(S/L)	Elongation Ratio(I/L)	S/I	(L-I)/(L-S)	Flatness %	OPI	MPSI	Roundness	Sphericity	Depositional Environment
LF-22	37.2	26.4	18	27.2	0.484	0.71	0.682	0.563	48.387	-12.5	0.691	0.6	0.7	Fluvial
LF-23	50.4	31.6	14.1	32.033	0.28	0.627	0.446	0.518	27.976	-3.581	0.5	0.7	0.5	Beach
LF-24	36.1	34.4	24.2	31.567	0.67	0.953	0.703	0.143	67.036	71.429	0.778	0.8	0.8	Fluvial
LF-25	48.1	22.9	14.3	28.433	0.297	0.476	0.624	0.746	29.73	-49.112	0.57	0.6	0.6	Beach
LF-26	52.9	26.1	17.6	32.2	0.333	0.493	0.674	0.759	33.27	-51.841	0.608	0.5	0.6	Beach
LF-27	34.1	28.8	20.2	27.7	0.592	0.845	0.701	0.381	59.238	23.741	0.746	0.5	0.7	Fluvial
LF-28	39	30	26	31.667	0.667	0.769	0.867	0.692	66.667	-38.462	0.833	0.6	0.8	Fluvial
LF-29	39.4	29.9	14.7	28	0.373	0.759	0.492	0.385	37.31	23.077	0.568	0.6	0.6	Beach
LF-30	40.6	31.9	26.3	32.933	0.648	0.786	0.824	0.608	64.778	-21.678	0.811	0.6	0.8	Fluvial
LF-31	35.9	26	15.9	25.933	0.443	0.724	0.612	0.495	44.29	1	0.647	0.6	0.7	Fluvial
LF-32	42.2	28.3	19.8	30.1	0.469	0.671	0.7	0.621	46.919	-24.107	0.69	0.5	0.7	Fluvial

Table 4: Pebble Morphometric Data of Samples from Ndeji

PEBBLE No	L(mm)	I(mm)	S(mm)	Mean (mm)	Flatness Ratio(S/L)	Elongation Ratio(I/L)	S/I	(L-I)/ (L-S)	Flatness %	OPI	MPSI	Roundness	Sphericity	Depositional Environment
NDJ-1	122	115	65	100.667	0.533	0.943	0.565	0.123	53.279	75.439	0.67	0.6	0.7	Fluvial
NDJ-2	102	101	43	82	0.422	0.99	0.426	0.017	42.157	96.61	0.564	0.7	0.6	Beach
NDJ-3	125	113	93	110.333	0.744	0.904	0.823	0.375	74.4	25	0.849	0.7	0.8	Fluvial
NDJ-4	83	77	61	73.667	0.735	0.928	0.792	0.273	73.494	45.455	0.835	0.6	0.8	Fluvial
NDJ-5	94	91	74	86.333	0.787	0.968	0.813	0.15	78.723	70	0.862	0.7	0.8	Fluvial
NDJ-6	131	125	93	116.333	0.71	0.954	0.744	0.158	70.992	68.421	0.808	0.6	0.8	Fluvial
NDJ-7	95	91	73	86.333	0.768	0.958	0.802	0.182	76.842	63.636	0.851	0.2	0.8	Fluvial
NDJ-8	93	91	63	82.333	0.677	0.978	0.692	0.067	67.742	86.667	0.777	0.3	0.7	Fluvial
NDJ-9	103	101	82	95.333	0.796	0.981	0.812	0.095	79.612	80.952	0.865	0.1	0.8	Fluvial
NDJ-10	98	95	82	91.667	0.837	0.969	0.863	0.188	83.673	62.5	0.897	0.2	0.8	Fluvial
NDJ-11	85	77	55	72.333	0.647	0.906	0.714	0.267	64.706	46.667	0.773	0.2	0.8	Fluvial
NDJ-12	74	73	52	66.333	0.703	0.986	0.712	0.045	70.27	90.909	0.794	0.8	0.8	Fluvial
NDJ-13	73	72	43	62.667	0.589	0.986	0.597	0.033	58.904	93.333	0.706	0.6	0.7	Fluvial
NDJ-14	63	62	54	59.667	0.857	0.984	0.871	0.111	85.714	77.778	0.907	0.7	0.8	Fluvial
NDJ-15	85	82	63	76.667	0.741	0.965	0.768	0.136	74.118	72.727	0.829	0.5	0.8	Fluvial
NDJ-16	71	63	45	59.667	0.634	0.887	0.714	0.308	63.38	38.462	0.768	0.2	0.7	Fluvial
NDJ-17	69	65	58	64	0.841	0.942	0.892	0.364	84.058	27.273	0.909	0.4	0.8	Fluvial
NDJ-18	85	85	65	78.333	0.765	1	0.765	0	76.471	100	0.836	0.5	0.8	Fluvial
NDJ-19	71	63	51	61.667	0.718	0.887	0.81	0.4	71.831	20	0.835	0.6	0.8	Fluvial
NDJ-20	60	42	22	41.333	0.367	0.7	0.524	0.474	36.667	5.263	0.577	0.7	0.6	Beach
NDJ-21	69	58	51	59.333	0.739	0.841	0.879	0.611	73.913	-22.222	0.866	0.8	0.8	Fluvial
NDJ-22	74	65	45	61.333	0.608	0.878	0.692	0.31	60.811	37.931	0.749	0.3	0.7	Fluvial
NDJ-23	68	65	53	62	0.779	0.956	0.815	0.2	77.941	60	0.86	0.2	0.8	Fluvial

Table 5. Pebble Morphometric Data of Samples from Gbugbu

PEBBLE No	L	I	S	Mean(mm)	Flatness Ratio(S/L)	Elongation Ratio(I/L)	S/I	(L-I)/ (L-S)	Flatness %	OPI	MPSI	Roundness	Sphericity	Depositional Environment
GB-1	75.1	35.1	34.4	48.2	0.458	0.467	0.98	0.983	45.806	-96.56	0.766	0.5	0.7	Fluvial
GB-2	55.9	40.6	26.7	41.067	0.478	0.726	0.658	0.524	47.764	-4.795	0.68	0.9	0.7	Fluvial
GB-3	44.8	42.4	30.1	39.1	0.672	0.946	0.71	0.163	67.188	67.347	0.781	0.9	0.7	Fluvial
GB-4	67.7	46	39.2	50.967	0.579	0.679	0.852	0.761	57.903	-52.281	0.79	0.7	0.7	Fluvial
GB-5	46.2	37.1	31.5	38.267	0.682	0.803	0.849	0.619	68.182	-23.81	0.833	0.9	0.7	Fluvial
GB-6	69	31.5	31.1	43.867	0.451	0.457	0.987	0.989	45.072	-97.889	0.763	0.8	0.7	Fluvial
GB-7	67.5	31.6	30.8	43.3	0.456	0.468	0.975	0.978	45.63	-95.64	0.763	0.9	0.7	Fluvial
GB-8	56.5	35.2	33.5	41.733	0.593	0.623	0.952	0.926	59.292	-85.217	0.826	0.4	0.8	Fluvial
GB-9	73.3	45.5	34.3	51.033	0.468	0.621	0.754	0.713	46.794	-42.564	0.707	0.5	0.7	Fluvial
GB-10	58.3	32	13.8	34.7	0.237	0.549	0.431	0.591	23.671	-18.202	0.467	0.9	0.6	Beach
GB-11	58.4	43.7	16.4	39.5	0.281	0.748	0.375	0.35	28.082	30	0.472	0.8	0.6	Beach
GB-12	50.5	36.2	17.7	34.8	0.35	0.717	0.489	0.436	35.05	12.805	0.555	0.5	0.6	Beach
GB-13	45	31.8	17.8	31.533	0.396	0.707	0.56	0.485	39.556	2.941	0.605	0.9	0.6	Beach
GB-14	64.8	41.3	26	44.033	0.401	0.637	0.63	0.606	40.123	-21.134	0.632	0.7	0.6	Beach
GB-15	35.5	29	17.4	27.3	0.49	0.817	0.6	0.359	49.014	28.177	0.665	0.7	0.7	Fluvial
GB-16	51.2	37.5	27.5	38.733	0.537	0.732	0.733	0.578	53.711	-15.612	0.733	0.4	0.7	Fluvial

PEBBLE No	L	I	S	Mean(mm)	Flatness Ratio(S/L)	Elongation Ratio(I/L)	S/I	(L-I)/ (L-S)	Flatness %	OPI	MPSI	Roundness	Sphericity	Depositional Environment
GB-17	65.8	41.1	26.4	44.433	0.401	0.625	0.642	0.627	40.122	-25.381	0.636	0.9	0.6	Beach
GB-18	51.4	37	18.7	35.7	0.364	0.72	0.505	0.44	36.381	11.927	0.569	0.9	0.6	Beach
GB-19	51.5	37.9	16.8	35.4	0.326	0.736	0.443	0.392	32.621	21.614	0.525	0.9	0.6	Beach
GB-20	46.2	39.7	28	37.967	0.606	0.859	0.705	0.357	60.606	28.571	0.753	0.4	0.7	Fluvial
GB-21	51.7	40.1	20.6	37.467	0.398	0.776	0.514	0.373	39.845	25.402	0.589	0.9	0.6	Beach
GB-22	41.5	37.2	21.3	33.333	0.513	0.896	0.573	0.213	51.325	57.426	0.665	0.7	0.7	Fluvial
GB-23	45.1	30.9	22.4	32.8	0.497	0.685	0.725	0.626	49.667	-25.11	0.711	0.9	0.7	Fluvial
GB-24	56.2	51.6	20	42.6	0.356	0.918	0.388	0.127	35.587	74.586	0.517	0.9	0.6	Beach
GB-25	58.8	43.9	20.5	41.067	0.349	0.747	0.467	0.389	34.864	22.193	0.546	0.8	0.6	Beach
GB-26	53.1	38.1	27.2	39.467	0.512	0.718	0.714	0.579	51.224	-15.83	0.715	0.3	0.7	Fluvial
GB-27	45.1	38.7	20.1	34.633	0.446	0.858	0.519	0.256	44.568	48.8	0.614	0.7	0.6	Beach
GB-28	53.7	37.1	24.8	38.533	0.462	0.691	0.668	0.574	46.182	-14.879	0.676	0.8	0.7	Fluvial
GB-29	73.6	45.9	29.7	49.733	0.404	0.624	0.647	0.631	40.353	-26.196	0.639	0.9	0.6	Beach
GB-30	64.7	45.6	38.4	49.567	0.594	0.705	0.842	0.726	59.351	-45.247	0.794	0.7	0.7	Fluvial
GB-31	50.5	33.6	25.9	36.667	0.513	0.665	0.771	0.687	51.287	-37.398	0.734	0.8	0.7	Fluvial
GB-32	45.9	34.9	26.3	35.7	0.573	0.76	0.754	0.561	57.298	-12.245	0.756	0.9	0.7	Fluvial
GB-33	47.8	37	22.8	35.867	0.477	0.774	0.616	0.432	47.699	13.6	0.665	0.9	0.7	Fluvial
GB-34	46.4	32.5	20.7	33.2	0.446	0.7	0.637	0.541	44.612	-8.171	0.657	0.9	0.7	Fluvial
GB-35	52.6	31.6	17.3	33.833	0.329	0.601	0.547	0.595	32.89	-18.98	0.565	0.7	0.6	Beach
GB-36	43.6	43.5	16.5	34.533	0.378	0.998	0.379	0.004	37.844	99.262	0.524	0.1	0.6	Beach
GB-37	54.5	34.8	16.7	35.333	0.306	0.639	0.48	0.521	30.642	-4.233	0.528	0.5	0.6	Beach
GB-38	46	36.1	20.1	34.067	0.437	0.785	0.557	0.382	43.696	23.552	0.624	0.9	0.7	Fluvial
GB-39	47.3	32.8	23.1	34.4	0.488	0.693	0.704	0.599	48.837	-19.835	0.701	0.9	0.7	Fluvial
GB-40	46.7	23.8	22.4	30.967	0.48	0.51	0.941	0.942	47.966	-88.477	0.767	0.9	0.7	Fluvial
GB-41	41.4	37.4	30.4	36.4	0.734	0.903	0.813	0.364	73.43	27.273	0.842	0.7	0.8	Fluvial

Table 6. Pebble Morphometric Data of Samples from Maganiko

PEBBLE No	L	I	S	Mean (mm)	Flatness Ratio(S/L)	Elongation Ratio(I/L)	S/I	(L-I)/ (L-S)	Flatness %	OPI	MPSI	Roundness	Sphericity	Depositional Environment
MG-1	57	45.9	31.3	44.733	0.549	0.805	0.682	0.432	54.912	13.619	0.721	0.74	0.7	Fluvial
MG-2	64.5	40.4	31.9	45.6	0.495	0.626	0.79	0.739	49.457	-47.853	0.731	0.7	0.7	Fluvial
MG-3	120.4	50.5	36.6	69.167	0.304	0.419	0.725	0.834	30.399	-66.826	0.604	0.6	0.6	Beach
MG-4	127.2	50.7	49.9	75.933	0.392	0.399	0.984	0.99	39.23	-97.93	0.728	0.6	0.7	Fluvial
MG-5	70.2	52.1	22	48.1	0.313	0.742	0.422	0.376	31.339	24.896	0.51	0.7	0.6	Beach
MG-6	112.5	51.3	31.6	65.133	0.281	0.456	0.616	0.756	28.089	-51.298	0.557	0.5	0.6	Beach
MG-7	61.7	41.3	34.5	45.833	0.559	0.669	0.835	0.75	55.916	-50	0.776	0.6	0.7	Fluvial
MG-8	90.6	66.6	46.9	68.033	0.518	0.735	0.704	0.549	51.766	-9.84	0.714	0.6	0.7	Fluvial
MG-9	69.7	41.8	41.2	50.9	0.591	0.6	0.986	0.979	59.11	-95.789	0.835	0.7	0.8	Fluvial
MG-10	90.4	58.2	27.3	58.633	0.302	0.644	0.469	0.51	30.199	-2.06	0.521	0.5	0.6	Fluvial
MG-11	73.5	54.7	33.5	53.9	0.456	0.744	0.612	0.47	45.578	6	0.654	0.6	0.7	Fluvial
MG-12	63.6	50.9	24.8	46.433	0.39	0.8	0.487	0.327	38.994	34.536	0.575	0.6	0.6	Beach
MG-13	59.4	53.9	28.5	47.267	0.48	0.907	0.529	0.178	47.98	64.401	0.633	0.6	0.6	Beach
MG-14	75.7	71.1	58	68.267	0.766	0.939	0.816	0.26	76.618	48.023	0.855	0.7	0.8	Fluvial
MG-15	108.6	95.5	38.7	80.933	0.356	0.879	0.405	0.187	35.635	62.518	0.525	0.5	0.6	Beach
MG-16	85.4	77.8	35.2	66.133	0.412	0.911	0.452	0.151	41.218	69.721	0.571	0.5	0.6	Beach
MG-17	79.9	60.3	33.6	57.933	0.421	0.755	0.557	0.423	42.053	15.335	0.617	0.6	0.6	Beach
MG-18	49.9	46.2	40.6	45.567	0.814	0.926	0.879	0.398	81.363	20.43	0.894	0.7	0.8	Fluvial
MG-19	92.3	46	20.6	52.967	0.223	0.498	0.448	0.646	22.319	-29.149	0.464	0.5	0.6	Beach
MG-20	77.8	34.3	26.4	46.167	0.339	0.441	0.77	0.846	33.933	-69.261	0.639	0.6	0.6	Beach
MG-21	53.7	26.1	19.8	33.2	0.369	0.486	0.759	0.814	36.872	-62.832	0.654	0.6	0.7	Fluvial
MG-22	43.6	38.9	34.7	39.067	0.796	0.892	0.892	0.528	79.587	-5.618	0.892	0.7	0.8	Fluvial
MG-23	52	46.2	34.6	44.267	0.665	0.888	0.749	0.333	66.538	33.333	0.793	0.6	0.7	Fluvial
MG-24	93.6	80.3	42.8	72.233	0.457	0.858	0.533	0.262	45.726	47.638	0.625	0.5	0.6	Beach
MG-25	69.2	44.5	38.5	50.733	0.556	0.643	0.865	0.805	55.636	-60.912	0.784	0.6	0.7	Fluvial
MG-26	55.2	43.1	19.1	39.133	0.346	0.781	0.443	0.335	34.601	32.964	0.535	0.5	0.6	Beach

PEBBLE No	L	I	S	Mean (mm)	Flatness Ratio(S/L)	Elongation Ratio(I/L)	S/I	(L-I)/ (L-S)	Flatness %	OPI	MPSI	Roundness	Sphericity	Depositional Environment
MG-27	52.7	50.4	43.9	49	0.833	0.956	0.871	0.261	83.302	47.727	0.899	0.7	0.8	Fluvial
MG-28	43.5	34.7	26.7	34.967	0.614	0.798	0.769	0.524	61.379	-4.762	0.779	0.7	0.8	Fluvial
MG-29	52.6	45.9	44.5	47.667	0.846	0.873	0.969	0.827	84.601	-65.432	0.936	0.7	0.9	Fluvial
MG-30	100.3	67.6	61.2	76.367	0.61	0.674	0.905	0.836	61.017	-67.263	0.821	0.7	0.8	Fluvial
MG-31	68.9	62.3	30.5	53.9	0.443	0.904	0.49	0.172	44.267	65.625	0.601	0.6	0.6	Beach
MG-32	53.8	26.5	21.2	33.833	0.394	0.493	0.8	0.837	39.405	-67.485	0.681	0.6	0.7	Fluvial
MG-33	122.2	52.1	41.7	72	0.341	0.426	0.8	0.871	34.124	-74.161	0.649	0.6	0.7	Fluvial
MG-34	64.4	47.4	24.9	45.567	0.387	0.736	0.525	0.43	38.665	13.924	0.588	0.5	0.6	Beach
MG-35	60.8	39.9	38.3	46.333	0.63	0.656	0.96	0.929	62.993	-85.778	0.846	0.7	0.8	Fluvial
MG-36	59.9	35.2	18.3	37.8	0.306	0.588	0.52	0.594	30.551	-18.75	0.542	0.5	0.6	Beach
MG-37	120.8	117	48.5	95.433	0.401	0.969	0.415	0.053	40.149	89.488	0.55	0.5	0.6	Beach
MG-38	109.2	65.1	62.3	78.867	0.571	0.596	0.957	0.94	57.051	-88.06	0.817	0.7	0.8	Fluvial
MG-39	95.3	69.5	32.6	65.8	0.342	0.729	0.469	0.411	34.208	17.703	0.543	0.6	0.6	Beach
MG-40	47.5	44.2	32.1	41.267	0.676	0.931	0.726	0.214	67.579	57.143	0.789	0.7	0.8	Fluvial
MG-41	35.8	31.6	28.6	32	0.799	0.883	0.905	0.583	79.888	-16.667	0.898	0.8	0.9	Fluvial
MG-42	32.6	31.6	30.9	31.7	0.948	0.969	0.978	0.588	94.785	-17.647	0.975	0.8	0.9	Fluvial
MG-43	52.1	46.6	45.9	48.2	0.881	0.894	0.985	0.887	88.1	-77.419	0.954	0.8	0.9	Fluvial
MG-44	70.2	52.9	29.8	50.967	0.425	0.754	0.563	0.428	42.45	14.356	0.621	0.6	0.6	Beach
MG-45	60.9	58	35.4	51.433	0.581	0.952	0.61	0.114	58.128	77.255	0.708	0.7	0.7	Fluvial
MG-46	61.8	47.4	26.3	45.167	0.426	0.767	0.555	0.406	42.557	18.873	0.618	0.6	0.6	Beach
MG-47	64.8	53.1	36.5	51.467	0.563	0.819	0.687	0.413	56.327	17.314	0.729	0.7	0.7	Fluvial
MG-48	70.9	46.8	37.9	51.867	0.535	0.66	0.81	0.73	53.456	-46.061	0.756	0.6	0.7	Fluvial
MG-49	66.4	42.8	38.6	49.267	0.581	0.645	0.902	0.849	58.133	-69.784	0.806	0.7	0.8	Fluvial
MG-50	57.7	52.5	42.9	51.033	0.744	0.91	0.817	0.351	74.35	29.73	0.847	0.7	0.8	Fluvial
MG-51	55.7	47.9	24.5	42.7	0.44	0.86	0.511	0.25	43.986	50	0.608	0.6	0.6	Beach
MG-52	54.7	32.2	18.8	35.233	0.344	0.589	0.584	0.627	34.369	-25.348	0.585	0.5	0.6	Beach
MG-53	92.7	76.8	38.1	69.2	0.411	0.828	0.496	0.291	41.1	41.758	0.589	0.6	0.6	Beach

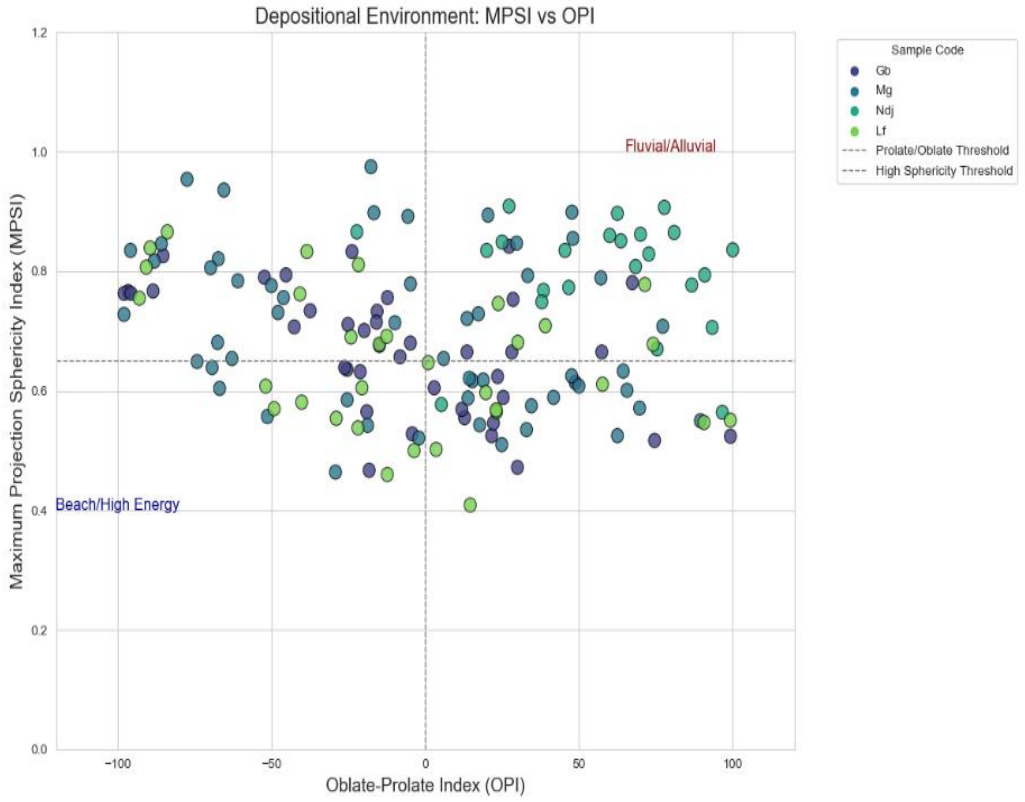

Figure 11: Bivariate Plot of MPSI Vs. OPI (after Stratten, 1973)

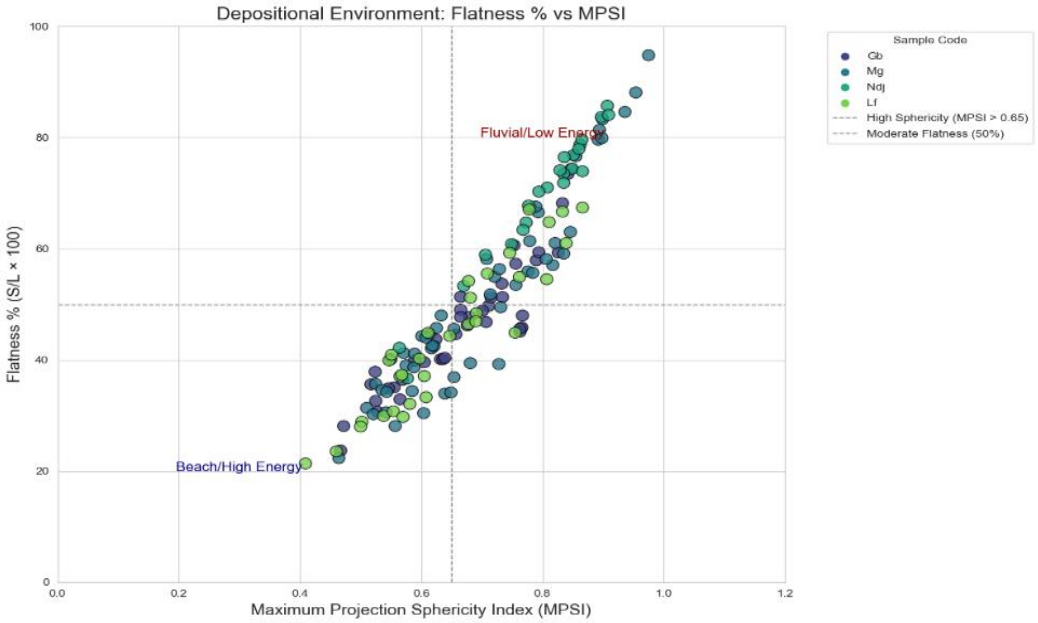

Figure 12: Bivariate Plot of Flatness Against MPSI (after Stratten, 1973)

Pebble Shape and Transportation History

The Sphericity-Form diagram of Sneed and Folk (1958) (Figure 13) provides insights into pebble shape, transport history and depositional environments across the locations. Most of the pebbles plotted within the bladed (B), while a few pebbles fall within the compact bladed (CB), compact platy (CP) elongated (E), and very elongated (VE) zones (Figure 13). The dominance of bladed and platy forms with low to moderate sphericity, indicate short to moderate transportation history and low energy environments. The prevalence of bladed forms points to mechanical weathering (e.g., fracturing, cleavage), being dominant over hydraulic rounding, suggest immature sediments and proximally sourced with limited abrasion. MG pebbles showed the widest distribution across bladed to very elongated fields, suggesting variable transport energy and mixed depositional processes. GB pebbles are more clustered in the bladed zones, reflecting moderate sphericity and more uniform transport conditions. ND pebbles plot around the compact-platy (CP) and bladed (B) fields, implying lower sphericity and shorter transport distances or reworking in high-energy settings. In contrast, LF pebbles are mostly elongated and bladed, consistent with long-distance fluvial transport. These shape variations highlight differences in sedimentary processes and energy conditions that influenced pebble rounding and form across the study locations. The shape distributions reveal variations in the geological history and environmental conditions of each sampling location.

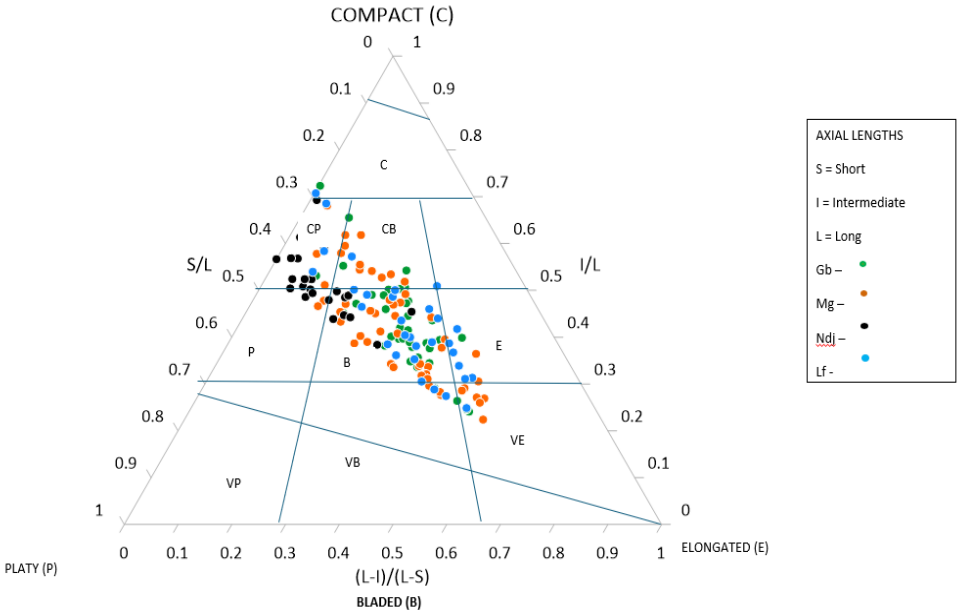

Figure 13: Sphericity-form Diagram of Sneed and Folk (1958) for the Pebbles. Most Pebbles Fall within the Bladed (B) zones with few in Elongate (E), Compact Bladed (CB), Compact Platy (CP) and Very Elongate (VE)

CONCLUSION

The grain size analysis conducted for the samples from Gbugbu, Ndeji, Maganiko and Lafiagi revealed significant variability in mean size, sorting, and skewness, indicating diverse energy conditions and depositional environments. The graphic mean values suggest energy conditions ranging from low (fine-grained sediments) to (coarser grains), which reflect both fluvial and beach tidal depositional settings. Poor sorting (as indicated by high standard deviation values) and varied skewness across all locations suggest fluctuating hydrodynamic conditions and complex sediment transportation processes. All sampled locations show platykurtic kurtosis, pointing to flat and broad grain-size distributions, typical of immature or reworked sediment sources. Pebble morphometry indicates a dominance of fluvial environments in most locations, supported by the bladed, compact-bladed, and elongated shapes of the pebbles. The occurrence of beach pebbles is an indication that the sediments were deposited in an environment shared between river and beach tidal zone since many of pebbles showed a bladed form.

REFERENCES

Adeleye D.R 1974: Sedimentology of the fluvial Bida sandstone (cretaceous) Nigeria. Sedimentary geology. 12, Pg1-24

Agyingi, C.M., (1993). Palynological evidence for a Late Cretaceous age for Patti Formation, eastern Bida Basin, Nigeria. *Journal of African Earth sciences.*17, 512–522.

Akande, S. O., Ojo, O. J., Erdtmann, B. D., *et al*. (2005). Paleoenvironments, Organic Petrology and Rock Eval

Akande, S. O., Ojo, O. J., Erdtmann, B. D., *et al*. (2005). Paleoenvironments, organic petrology and Rock-Eval studies on source rock facies of the Campanian to Maastrichtian Patti Formation, southern Bida basin, Nigeria. *Journal of African Earth Sciences*, 41, 394-406. http://dx.doi.org/10.1016/j.jafrearsci.2005.07.006

Amajor, L. C. & Ngerebara, O. D. (1990). Significance of Compositional and textural properties of sands from western Andoni Beach and flanking rivers (Andoni and Imo), eastern Niger Delta, Nigeria. *Journal of Mining Geology*, 26, 269-277.

Ayuba, . R., Baba, . Y., Adamu, . L. M., Ochu, . G. D., Ebe, . A., & Emmanuel, . A. U. (2024). Geochemical, Mineralogical, and Petrographical studies of ironstones around Mount Patti, Southern Bida Basin, Nigeria: Implications for quality assessment, provenance and environment of deposition. *Fudma Journal of Sciences*, *8*(1), 45-55. https://doi.org/10.33003/fjs-2024-0801-2251

Bamidele, T.E., Ojo, O.J., (2025). Geochemical, diagenetic, and depositional characteristics of the Maastrichtian Agbaja Formation ironstone exposed at Enegbaki, southern Bida Basin, Nigeria. *Results in Earth Sciences*. 3, 100118. https://doi.org/10.1016/j.rines.2025.100118.

Braide, S. P. (1992a). Geological development, origin, and energy mineral resources potential of the Lokoja Formation in the southern Bida Basin. *Journal of Mining and Geology*, 28, 33-44.

Braide, S. P. (1992b). Syntectonic fluvial sedimentation in the central Bida Basin. *Journal of Mining and Geology*, 28, 55-64.

Dobkins, J. E. & Folk, R. L. (1970). Shape development on Tahiti – Nui. *Journal of Sedimentary Petrology*, 40, 1167-1203.

Folk, R. L. & Ward, W. C. (1957). Brazo River bar: A study in the significance of grain size parameters. *Journal of Sedimentary Petrology*, 27, 3-26

Freidman, G. M. (1979). Differences in size distribution of populations of particles among sands of various origin. *Sedimentology*, 20, 3-32. http://dx.doi.org/10.1111/j.13653091.1979.tb00336.x

Friedman, G. M. (1967). Dynamic processes and statistical parameters compared for size frequency distribution of beach and river sands. *Journal of sedimentary Petrology*, 37, 327-354.

Idowu, J. O., & Enu, E. I. (1992). Petroleum geochemistry of some late Cretaceous shale from the LokojaSandstone of Middle Niger Basin, Nigeria. *Journal of African Earth Sciences*, 14, 443-455.http://dx.doi.org/10.1016/0899-5362(92)90047-G

Luttig, G. (1962). The shape of pebbles in the continental fluviatile and marine facies. *Int. assoc. Scientific hydrology pub*. 59, 235-258.

Madi, K., Ndlazi, N.Z. (2020). Pebble morphometric analysis as signatures of the fluvial depositional environment of the Katberg Formation near Kwerela River around East London, Eastern Cape Province, South Africa. *Arabian Journal of Geosciences* 13, 235. https://doi.org/10.1007/s12517-020-5189-z

Nwajide, C. S. & Hoque, M. (1982). Pebble morphometry as an aid in environmental diagnosis: an example from the middle BenueTrough Nigeria. *Journal of Mining and Geology*, 19, 114-120.

Obaje, N. G., Wehner, H., Scheeder, G., *et al*. (2004). Hydrocarbon prospectivity of Nigeria's inland basins from the viewpoint of organic geochemistry and organic petrology. *American Association of Petroleum Geologists Bulletin*, 88, 325-353.

Ojo, O. J & Akande, S. O. (2009). Sedimentology and depositional environments of the Maastrichtian Patti Formation, southeastern Bida Basin, Nigeria. *Cretaceous Research*, 30, 1415-1425. http://dx.doi.org/10.1016/j.cretres.2009.08.006

Ojo, O. J. & Akande, S. O. (2003). Facies Relationships and Depositional Environments of the Upper Cretaceous Lokoja Formation in the Bida Basin, Nigeria. *Journal of Mining and Geology*, 39, 39-48. http://dx.doi.org/10.4314/jmg.v39i1.18789

Ojo, O.J, Adepoju, S.A, Awe, A, Adeoye, M.O, Olumayade, E.G, Ndukwe, O.S, Abdulraman, S.O, Haruna, K.A and Jimoh, A.Y (2026). Uncovering the Late Cretaceous paleoenvironment and paleoclimate of the Agbaja Plateau, Bida Basin, Nigeria: An inorganic geochemical analysis of

shales and implications for organic matter enrichment. *Geosystems and Geoenvironment*. 5(1). 100452, ISSN 2772-8838, https://doi.org/10.1016/j.geogeo.2025.100452.

Ojo, O.J, Jimoh, A.Y., Umelo, J.C., Akande, S.O. (2020). Organic geochemical and palynological studies of the Maastrichtian source rock intervals in Bida Basin, Nigeria: Implications for hydrocarbon prospectivity. Journal of Petroleum Exploration and Production Technology 10, 3191–3206. https://doi.org/10.1007/s13202- 020- 00989- z

Ojo, O.J., (2012). Depositional Environments and Petrographic Characteristics of Bida Formation around Share-Pategi, Northern Bida Basin, Nigeria. Journal of Geography and Geology. 4(1), 224-241.

Ojo, O.J., and Akande, S.O., (2006). Sedimentological and palynological studies of the Patti Formation, Southeastern Bida Basin, Nigeria: Implications for paleoenvironments and paleogeography. *Nig. Ass. Pet. Expl. Bull*. 19(1), 61–77.

Ojo, O.J., Bamidele, T.E., Adepoju, S.A., Akande, S.O. (2021). Genesis and paleoenvironmental analysis of the ironstone facies of the Maastrichtian Patti Formation, Bida Basin, Nigeria. *Journal of African Earth Sciences*, 174. 104058pp. doi: https://doi.org/10.1016/j.jafrearsci.2020.104058.

Ojoma, P. E., Martins, O. A., Ayinla, H. A., Obasi, I. A., & Simon, D. C. (2024). Field occurrence and compositional characteristics of the clay horizon in the Patti Formation, Southern Bida Basin North-Central Nigeria. *Fudma Journal of Sciences*, *8*(5), 79-88. https://doi.org/10.33003/fjs-2024-0805-2696

Olaniyan, O., & Olabaniyi, S. B. (1996). Facies analysis of the Bida Sandstone Formation around Kajita, Nupe Basin, Nigeria. *Journal of African Earth Sciences*, 23, 253-256. http://dx.doi.org/10.1016/S0899-5362(96)00066-8

Olugbemiro, R. & Nwajide, C. S. (1997). Grain size distribution and particle morphogenesis as signatures of depositional environments of Cretaceous (non-ferruginous) facies in the Bida Basin, Nigeria. *Journal of Mining and Geology*, 33, 89-101.

Selley, R. C. (1985). Ancient Sedimentary Environment, third ed. *Cornell University Press, Ithaca, NY*, 317p.

Sneed, E. D. & Folk, R. L. (1958). Pebbles in the lower Colorado River, Texas: a study in particles morphogenesis. *Journal of Sedimentary Petrology*, 66, 114-150.

Stratten, J. (1973). Notes on the application of shape parameters to differentiate between beach and river deposits in southern Africa. *Trans Geolo. Soc. S. Africa*, 76, 59-64.

Tucker, M. E. (1988). Sedimentary Petrology, *Blackswell ScientificPublication, Great Britain*, 235p.

Udensi, E. E. & Osasuwa, I. B. (2004). Spectra determination of depths to magnetic rocks under the Nupe Basin, Nigeria. *Nigeria Association of Petroleum Explorationists Bulletin*, 17, 22-37.